Carbon-based Nanodevices for Electronic and Optical Applications

Anupama B. Kaul[*], Krikor Megerian[*], Leif Bagge[*, **], Henry G. LeDuc[*], Larry Epp[*], James B. Coles[*], Michael Eastwood[*], and Marc Foote[*]

[*]Jet Propulsion Laboratory, California Institute of Technology, Pasadena, California 91109
[**]Department of Electrical and Computer Engineering, University of Texas, Austin, TX 78712

ABSTRACT

Carbon-based nanomaterials have been actively applied to a diverse array of space-based applications in electronics and optics at the Jet Propulsion Laboratory. In the area of nano-electro-mechanical-systems (NEMS), we describe the implementation of carbon nanotubes (CNTs) and carbon nanofibers (CNFs) to dc nanorelays, as well as for AC resonator applications, which are under consideration for extreme environment electronics. We have also implemented single-walled nanotubes (SWNTs) to physical sensing, specifically for forming miniaturized pressure sensors for vacuum micro-cavity applications, where the mechanism of operation in such sensors relies on the thermal conductivity principle. Finally, we have also initiated an effort to apply arrays of vertically oriented CNTs for optical applications, specifically to act as broad-band optical absorbers for calibration targets. In this paper, we provide an overview of the recent results in each of these three applications of carbon nanomaterials.

Keywords: carbon nanomaterials, CNTs, CNFs, nanoelectronics, optical absorbers

1 INTRODUCTION

Low-dimensional carbon-based nanomaterials, such as carbon nanotubes (CNTs), carbon nanofibers (CNFs), graphene [1] and graphene nanoribbons [2] are gaining a great deal of attention for nanoelectronics, sensing and nanophotonics applications based on the unique and remarkable materials properties that carbon-based nanomaterials possess in general. We will describe our work conducted at the Jet Propulsion Laboratory, in developing novel devices based on one-dimensional (1D) CNTs and CNFs for nanoelectronic, sensing and optical applications. In nano-electro-mechanical-systems (NEMS), we are utilizing CNTs for dc nanorelays, as well as for AC resonators, which are under development for extreme environment electronics. These NEMS architectures rely on a vertical tube architecture to enable three-dimensional (3D) electronics applications of such carbon nanostructures. In the area of sensing, thermally-grown single-walled nanotubes (SWNTs) have been utilized for pressure sensors, potentially for micro-cavity applications. Such sensors operate on the thermal conductivity principle, where heat dissipation through the substrate is minimized by suspending the SWNTs in order to enhance pressure sensitivity. Finally, for optical applications, we have utilized arrays of vertically oriented tubes for broad-band optical absorbers which are under development for black-body calibration targets for spectrometers in order to enable higher sensitivity measurements for space-instruments.

2 APPLICATIONS

The application of 1D carbon-based nanomaterials in the area of NEMs or actuators, sensors and optical absorbers is described in more detail in Section 2.1, 2.2 and 2.3, respectively.

2.1 Actuators (NEMS)

In order to overcome the limitations of Si transistors as a result of shrinking device dimensions, NEM switches are gaining increasing attention due to their potential for low-power, high-speed and low-leakage current operation, as well as their potential for operability in harsh environments. Nanotube-based NEM switches have already been demonstrated for a variety of applications, [3,4,5,6], where the tubes were oriented parallel to the substrate. In this paper, we present an architecture where the tubes are oriented perpendicular to the substrate to potentially increase integration density of carbon-based nanomaterials for 3D-electronics. Switching between vertically oriented tubes arranged in a 3-terminal configuration was recently reported by Jang *et al.* [7]. Our CNFs were synthesized using dc plasma-enhanced (PE)

chemical vapor deposition (CVD), where a nanoprobe inside an SEM was used to actuate single tubes [8].

We have employed nanomanipulation to characterize the properties of individual, as-grown, vertically-oriented tubes, which suggests such structures have promise in nonvolatile memory applications. The SEM image in Fig. 1a shows a tube with a gap g_0 ~ 220 nm just before actuation, while the SEM in Fig. 1b shows the tube just after actuation. The switching or pull-in voltage in this case occurs at ~ 32 V (cycle 1) and ~ 35 V (cycle 2); since the contact length was < 50 nm, the tube detached from the probe prior to the onset of cycle 2. The turn-on transition was abrupt while the turn-off transition between cycle 1 and cycle 2 was identical and was dominated by the contact resistance. In general, the mechanical properties of the tubes were found to be extremely attractive for NEMS applications and we are currently progressing to form 3D NEMS switches which are comprised of monolithically integrated electrodes.

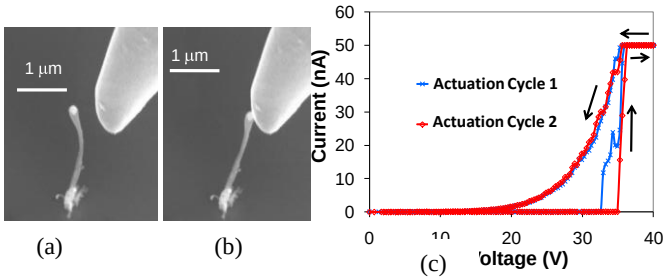

Figure 1. (a) A single tube that is within a few hundred nm of the nanoprobe on the right. (b) When voltage is applied on the nanoprobe, it causes the tube to electrostatically switch, and stick to the probe. (c) The switching I-V characteristic shows 2 switching cycles with V_{pi} ~ 32 V and 35 V, on cycle 1 and cycle 2, respectively. The switching I-V characteristic also shows the abruptness of the turn-on transition. Hysteresis in the I-V indicates stiction and suggests such structures are promising for three-dimensional nonvolatile memory applications.

We have also extended this work to consider utilizing vertically oriented tubes for mechanical resonators. This has been initiated, where an AC model was developed using COMSOL Multiphysics, which is a commercially available finite-element-simulator. The electro-mechanical coupling of the CNT was examined as a function of an incoming AC signal on a probe in close proximity to the tube. The modeling results confirmed that the mechanical resonance was maximized when the frequency of the input signal was equal to the first order harmonic of the CNT. The AC capacitance of the CNT varied near the first resonant mode, and was approximately constant above and below this frequency. This characteristic was studied as a function of the DC bias solution, where the AC signal had an amplitude V_{AC} = 1 V. Simulations of the AC capacitance of the system showed that for DC biases less than ~ 100 mV, no change in AC capacitance was found. These results are illustrated in Figure 2 below and suggests the variation of the AC capacitance with DC bias behaves in a manner similar to a gating voltage.

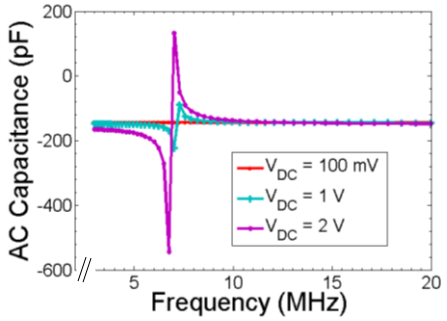

Figure 2. The AC capacitance calculated for a NEMS resonator based on a single vertically oriented tube as a function of frequency for several DC biases with V_{ac} = 1 V. When V_{DC} < 100 mV, no AC capacitance is detected.

An investigation of the resonance frequency was also performed for various geometrical parameters of our 3D NEMS architecture. An example of the variation of amplitude with probe-to-tube gap G is shown in Figure 3, which indicates the resonance amplitude scales inversely with gap G. In general, such resonators are of interest for communications and mass-sensing applications.

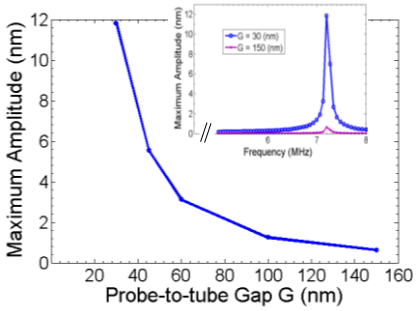

Figure 3. The frequency response of a 5 µm long CNT where g ranged from 30 nm – 150 nm, with V_{DC} = 0.1 V and V_{ac} = 1 V. The inset shows that the Q is higher when the gap is 30 nm when compared to 150 nm.

2.2 Sensors

In the second application area of sensing, we have formed miniaturized CNT-based pressure sensors which can be utilized with micro-cavities (vacuum micro-electronics, RF MEMS, gyroscopes, etc) [9,10]; a schematic of such a vacuum micro-cavity is shown in Figure 4. Such sensors have been reported to operate at low power (nW-µW) and exhibit a wide-dynamic range (760 Torr - 10^{-6} Torr). The ultra-miniature size of such sensors compared to conventional high vacuum sensors (e.g.

thermocouple, ion gauges), makes them nonintrusive and easily integratable with other vacuum-encased microdevices (e.g. MEMS gyroscopes, RF MEMS switches) and vacuum microtube oscillators and amplifiers; here, pressure changes over lifetime can effect device performance, and the magnitude of such changes can be especially large due to outgassing in small-volume micro-cavities.

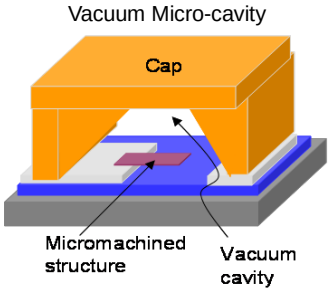

Figure 4. A micromachined structure inside a vacuum micro-cavity.

An SEM image of a fabricated SWNT sensor is shown in Fig. 5a, which shows a SWNT bridging the electrodes. The devices were tested prior to release, after annealing and after releasing from the SiO_2 substrate. The SWNTs were released from the SiO_2 substrate using Buffered-Oxide-Etch (BOE) and critical point drying. Shown in Fig. 5b is the pressure response for unannealed, annealed, as well as the annealed and released devices. In all three cases, the conductance of the CNT device decreased rapidly initially, after which point changes occur less rapidly. As pumping occurs, gas phase collisions cause thermal energy to be transferred to the gas, which results in local cooling, influencing the resistance of the current carrying element. Higher pressures generate higher collision rates and thus, greater cooling. Since the differential change of conductance with temperature is positive for our SWNTs, cooling would result in conductance suppression with decreasing pressure, as observed. Eventually, the gas-phase mean free paths become longer, and the response becomes less sensitive. For the unannealed and annealed device in Fig. 5b, the sensitivity is diminished beyond about 100 sec. (~ 1 Torr) but the released CNT gas sensor has a continued decrease in conductance well into the 10^{-6} Torr range. The data appears to confirm that by removing part of the SiO_2 substrate underneath the current carrying element, sensitivity is increased into the lower pressure ranges since solid-state conduction through the substrate is minimized, leaving more of the heat to be propagated by the gas.

The increase in sensitivity after substrate removal is better illustrated in Fig. 6 which shows the net current change (ΔI) for released and unreleased device in the pressure range of ~ 5 x 10^{-6} Torr to ~ 8 x 10^{-7} Torr. In both cases, ΔI increases with power but the released device has a three times larger change, where ΔI ~ 550 nA at a bias of ~ 6 μW, compared to ΔI ~ 150 nA for the unreleased device.

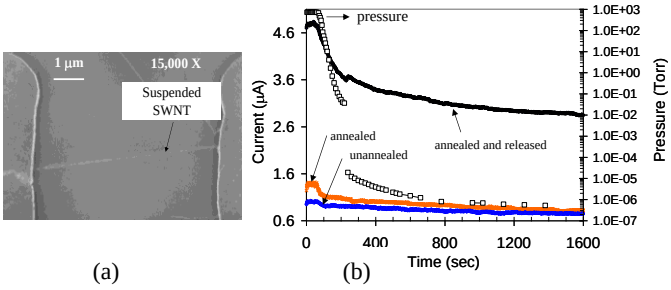

Figure 5. (a) SEM image showing a fully suspended tube after release using critical point drying in an IPA bath. Trench depth ~ 310 nm. (b) Absolute current variation for the unannealed, annealed, as well as the annealed and released devices as a function of time/pressure at a bias power of ~ 2 μW. The pressure response of the unannealed and annealed devices saturates beyond ~ 100 sec. or ~ 1 Torr, but the released device shows a measurable conductance change down to ~ 10^{-6} Torr.

While the increased current sensitivity with substrate removal can be explained on the basis of heat minimization through the substrate, the reduced dimensionality for phonon scattering in 1-D systems, in particular suspended SWNTs, can cause unique effects to arise at large bias voltages and power. At high fields a negative differential conductance regime was detected in our tubes which may explain the enhanced pressure sensitivity observed in suspended SWNTs at high bias voltages.

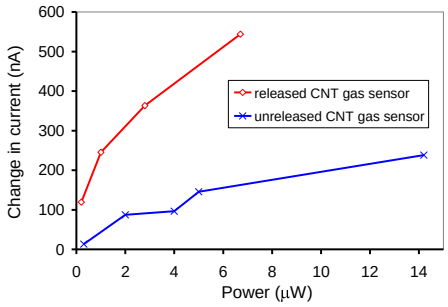

Figure 6. Net current change from ~ 5 x 10^{-6} Torr to ~ 8 x 10^{-7} Torr for the released and unreleased CNT gas sensor as a function of bias power. The largest change in conductance is for released device as power is increased.

2.3 Optical Absorbers

Finally, in the third application area, we will describe our work in developing optical absorbers based on vertically-oriented tubes which are gaining increasing attention as ideal black-bodies. The starting substrate on which our tubes were grow was typically a degenerately doped Si wafer (1 - 5 mΩ-cm) with Ni or Co catalyst, where the growth temperatures ranged from 500 - 700 ºC in the presence of acetylene (C_2H_2) and ammonia (NH_3), which served as the carbon feedstock and diluent gas, respectively. When the desired growth pressure had been attained, the discharge was ignited, and growth was carried

out for a fixed duration. More details of our growth chamber are provided in [11]. Shown in Fig. 7a is an SEM image of vertically oriented tubes formed using this technique.

The optical measurements were conducted using a high resolution, fiber coupled, spectroradiometer in a standard reflectance measurement experimental setup as follows. The sample was placed on a reference panel and a standard halogen light source was aimed at normal incidence to it. The bare fiber connector of the spectroradiometer was brought close to the sample such that the desired region of measurement completely filled the angle of view of the fiber face when oriented at a 20^{o} incident angle from normal to avoid obstructing the sample illumination. Relative reflectance spectra from 350nm - 2500nm were obtained by first white referencing the spectroradiometer to a 99% reflective Spectralon panel and optimizing the instrument integration time. Finally, the reflected light intensity from the sample under test was measured while avoiding changes to the geometry of the measurement system, yielding accurate reflectance spectra for each of the samples in the study. Shown in Fig. 7b is the response from the optical measurements for two CNT samples, Sample 1 and Sample 2, which appear to be promising. For example, CNT Sample 2 shows a total reflectance of ~ 0.1% up to ~1.2 μm, which increases only slightly up to 0.23 % at 2.5 μm. Metal-black appear to have a reflectance that is larger by at least a factor of five at these wavelengths.

(a)

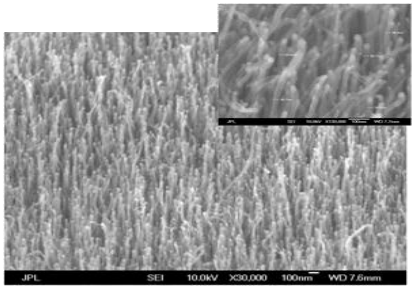

(b)

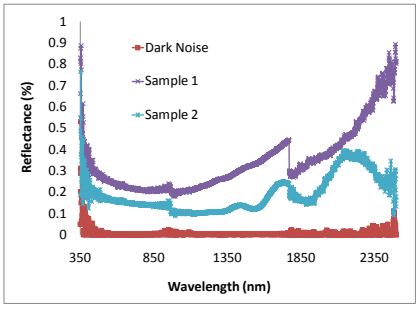

Figure 7. (a) An SEM image of vertically aligned tubes. The inset shows a high magnification image of CNTs indicating that they have typical diameters of ~ 25 nm. (b) Optical measurements conducted from 350 nm to 2.5 μm for two CNT samples comprising of vertically oriented tubes. Sample 2 has a low total reflectance of ~ 0.23% up to ~ 2.5 μm.

3 ACKNOWLDEGEMENTS

We would like to thank Robert Kowalczyk for making system modifications to the dc PECVD growth chamber, Eric Wong for thermal CVD growth (Fig. 6a), Choonsup Lee, Richard Baron and Paul von Allmen for useful discussions. This research was carried out at the Jet Propulsion Laboratory, California Institute of Technology, under a contract with the National Aeronautics and Space Administration and was funded through the internal Research and Technology Development (R&TD) program.

REFERENCES

[1] S. Novoselov, A. K. Geim, S. V. Morozov, D. Jiang, Y. Zhang, S. V. Dubonos, I. V. Grigorieva, and A. A. Firsov, *Science* **306**, 666 (2004).
[2] Y. W. Son, M. L. Cohen, and S. G. Louie, *Phys. Rev. Lett.* **97**, 216803 (2006).
[3] T. Rueckes, K. Kim, E. Joselevich, G. Y. Tseng, C. L. Cheung, and C. M. Lieber, *Science* **289**, 94 (2000).
[4] E. Dujardin, V. Derycke, M. F. Goffman, R. Lefevre, and J. P. Bourgoin, *Appl. Phys. Lett.* **87,** 193107-1 (2005).
[5] A. Eriksson, S. Lee, A. Sourab, A. Issacsson, R. Kaunisto, J. M. Kinaret, and E. E. B. Campbell, *Nano Lett.* **8**, 1224 (2008).
[6] A. B. Kaul, E. W. Wong, L. Epp, and B. D. Hunt, *Nano Lett.* **6**, 942 (2006).
[7] J. E. Jang, S. N. Cha, Y. Choi, G. A. J. Amaratunga, D. J. Kang, D. G. Hasko, J. E. Jung, and J. M. Kim, *Appl. Phys. Lett.* **87**, 163114 (2005).
[8] A. B. Kaul, A. Khan, L. Bagge, K. G. Megerian, H. G. LeDuc, and L. Epp, *Appl. Phys. Lett.* **95**, 093103, (2009).
[9] A. B. Kaul and H. M. Manohara, *IEEE Trans. on Nanotech.* **8**, 252 (2009).
[10] A. B. Kaul, *Nanotechnology* **20**, 155501 (2009).
[11] A. B. Kaul, K. Megerian, P. von Allmen, and R. L. Baron, *Nanotechnology* **20**, 075303 (2009).